A Variable Finite Element Model of the Overall Human Masticatory System for Evaluation of Stress Distributions during Biting and Bruxism

S. Martinez[1], J. Lenz[1], K. Schweizerhof[1], H. J. Schindler[2]

[1]Karlsruhe Institute of Technology, Institute of Mechanics, Research Group Biomechanics
[2]University of Heidelberg, Department of Prosthodontics

1 Abstract

Simulating the masticatory system during chewing, clenching and bruxism, requires the model to capture the dynamical behavior of its different components: the mandibula and maxilla, the temporomandibular joint (TMJ) including the articular disc and the surrounding cartilage layers, the teeth, the periodontal ligaments (PDL), and the muscles. A considerable amount of literature has been published on individual components separately [1, 2, 3]. This contribution incorporates these elements, besides own components, into a single FE model under conditions closer to reality. Hereby the simulation is a transient analysis where the dynamic behavior of the jaw is considered, and where the reaction forces in the teeth and the joints arise from contact instead of nodal forces or constraints. The TMJ has been modeled with geometrical structures and material properties as found in the literature [2] with ensuing additional adjustments. The material properties of the PDL are calibrated to obtain a realistic force-displacement behavior. Geometries for the jaw and teeth were obtained through a segmentation process. Jaw motion is governed by forces from the jaw opening and closing muscles which have been positioned following proposals in the literature and are represented by Hill type muscle models. Activation levels of the muscles were employed based on previous work of the authors [3]. Analyses are executed with the FE program LS-DYNA [4]. The model currently reproduces realistic motions of the jaw during opening and closing. Reaction forces for a variety of biting tasks show good agreement with the literature. The model provides insight into the significance, or lack thereof, of particular structures such as the posterior attachments of the disc and the suprahyoid muscles during various situations. The current and future goals are to determine the stress distributions in the mandible, disc, teeth, and PDL during clenching, grinding and chewing with differently sized boluses, also when dental implants are incorporated at different positions of the mandible.

2 Introduction

The human masticatory system is composed of several structures: the mandibula, the temporomandibular joint (TMJ), the teeth, the periodontal ligaments (PDL), and the muscles. A considerable amount of literature has been published on these individual components. The PDL has been analyzed with finite element (FE) models using different material assumptions [1]; the TMJ has been modeled as an articular disc with cartilage layers using a combination of FE and rigid body analysis [2]; finally the muscles' role has been studied through electromyography and optimization strategies [5]. These different components were incorporated into a single FE model within the scope of a cooperation with the Zebris company [6]. The model (Figure 1) presently undergoes further development under the supervision of medical professionals.

3 Materials and Methods

3.1 Model geometry and discretization

The segmentation software "Mimics Innovation Suite" [7] was used to obtain the geometry from the DVT-scans of a patient provided by the University of Greifswald. The geometry was further processed with the software "Geomagic Studio 12" [8] to obtain a compatible format and to clean defects obtained during the segmentation process. The preprocessor "Hypermesh 12" [9] was used to mesh the complete model. Mesh convergence analyses showed that more than 900.000 elements are required for the model in the symmetrical case (bilateral biting case). This number doubles when the complete model is used. In our model, the superior part of the cartilage of the fossa is constrained as well as the superior part of the periodontal ligament of the maxillar teeth. Forces on the model are a result of the activation of the muscles.

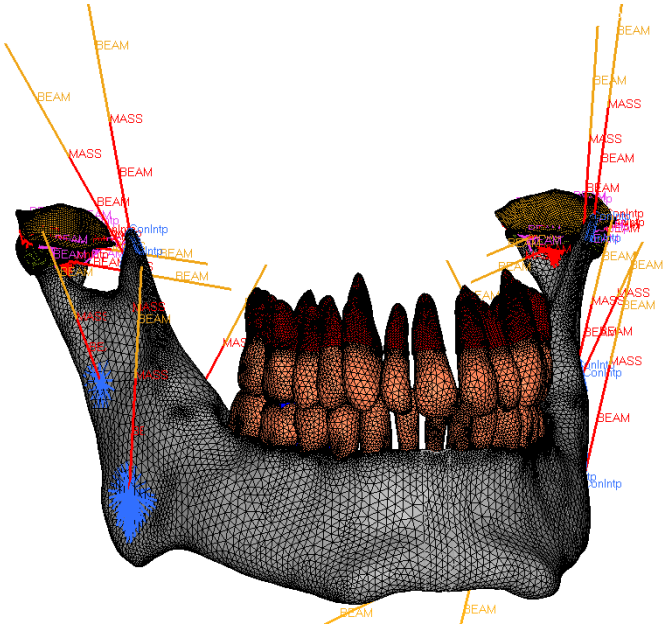

Fig.1: Complete model used for unilateral biting tasks.

3.2 Periodontal ligament

The periodontal ligament is the component that governs tooth mobility. From Nishira et al. [10], we can safely assume that the teeth undergo no deformation and act as rigid bodies due to their high stiffness. The central incisor tooth and its PDL were taken from our model and separately analyzed using different material parameters from several authors. We decided to ignore any work where linear elastic material models were used, since the PDL shows a highly non-linear behavior. Various authors [11, 12] calibrated material models to match the stress-strain results obtained from uniaxial tests on the PDL. Applying these material parameters proved unsatisfactory since the tooth displacements did not match the experimental results from Parfitt [13] and Lenz et al. [14]. Natali et al. [12] have material parameters that show good agreement with the force displacement curves but do not disclose them. Other authors implemented their own material models which produce results that closely match the results from the Parfitt experiment [15, 16]. In our study, it was decided to calibrate a hyperelastic material model available in most finite element codes.

A first order Ogden hyperelastic model showed the best fit with the stress-strain curves from the literature. Hyperelastic material models assume that the material behavior can be described by means of a strain energy function, from which the stress-strain relationship can be derived. In the case of the Ogden material model, the strain energy function is defined in LS-DYNA as

$$W = \sum_{i=1}^{3} \sum_{j=1}^{n} \frac{\mu_j}{\alpha_j} (\lambda_i^{\alpha_j} - 1) + K(J - 1 - \ln J) \tag{1}$$

where W is the strain energy potential, λ_i are the deviatoric principal stretches, μ_j, α_j, are material parameters, J is the determinant of the elastic deformation gradient and K the bulk modulus. The bulk modulus is computed using the Poisson's ratio.

The parameters that produced the best agreement with the experimental results for both vertical and horizontal loads were then selected and are presented in Table 1.

μ_1 [MPa]	α_1 [MPa]	v (Poissson's ratio)
2.50E-03	150	0.46

Table 1: Material parameters for the PDL.

The model was run as a quasi-static simulation in its initial phase. It is currently run as a dynamic problem which requires the incorporation of the dissipation properties exhibited by the PDL during the

initial phase of loading. Parameters for the viscous behavior of the PDL can be obtained e.g from Su et al. [17].

3.3 Temporomandibular joint (TMJ)

Several strategies have been employed to model the TMJ. The model of Koolstra & van Eijden [2] uses a combined finite element and rigid body analysis, where the joint consists of an articular disc and cartilage tissue represented with solid finite elements and the jaw is modeled as a rigid body. In this model, the disc is attached to the condyle by means of inextensible wires. The inextensible wires represent the lateral and medial attachments of the joint capsule. In the work of Perez & Doblare [18] a poroelastic material model is used to represent the disc, while the lateral and medial attachments are modeled directly as part of the geometry of the disc. The cartilage tissue is not taken into account in this model.
In our model, the TMJ consists of: the articular disc, the cartilage of the fossa, the cartilage of the condyle and the lateral, medial, posterior and anterior attachments of the disc. A Mooney-Rivlin hyperelastic material model whose parameters were obtained from Koolstra & van Eijden [2] is used for the cartilage and articular disc. The viscoelastic behaviour of the disc was also included, with the decay constants taken from Koolstra & van Eijden [19]. The decay constants that are outside of the time range of our problem were ignored.
Initially, the model only included the lateral and medial attachments, but the joint presented instabilities when the closing muscles were activated beyond a certain level. Disc displacement is notable during jaw opening and closing: The initial phase of the opening movement is primarily a rotation that progresses with an additional translational component; the inferior fibers of the retrodiscal tissue and the superior anterior attachments relax as the jaw opens, while the superior fibers of the retrodiscal tissue and the inferior anterior attachments become tense.
The inverse process can be observed during the closing process: The superior stratum of the retrodiscal tissue pulls the articular disc posteriorly while the superior head of the lateral pterygoid stabilizes the condyle. As the jaw closes, tension in the inferior stratum increases while decreasing in the superior stratum. Tension in the inferior stratum prevents anterior disc displacement in the case that the condyle moves too far distally.
To ensure joint stability -thus avoiding the instabilities mentioned above- during strong muscle forces, inclusion of the posterior and anterior attachments of the capsule is necessary. The mechanical properties of the retrodiscal tissue were studied by Tanaka et al. [20]. However, in this work only uniaxial tension tests were performed. This creates difficulties in the modeling process since the data of different types of tests are required to obtain stable solutions. As with the lateral and medial attachments, the anterior and posterior attachments were thus modeled using trusses with the elastic modulus following the stress-strain curve obtained by Tanaka [20].
The extent of the trusses was estimated from the area covered by the attachments on the disc. The area was further calibrated a) to ensure that the range of movement of the joint was not unrealistically limited, and b) at the same time to provide the stability required during strong muscle forces.

3.4 Cortical and cancellous bone

Two types of osseous tissue compose the bones: the cortical and the cancellous bone. The cortical bone supports the whole body and forms the outer shell of most bones. It is much denser, stronger and stiffer than cancellous bone. Values of Young's modulus of the bone vary between authors and depend on the type of test applied [21]. They also vary between subjects. Additionally, the cortical bone exhibits different elastic moduli in the longitudinal and radial directions with respect to the axis of the bone [22]. A linear elastic isotropic model was used in our simulations. Young's modulus and Poisson's ratio where taken from Tanaka et al. [23] and are shown in Table 2.

	Young's Modulus [MPa]	**v (Poissson's ratio)**
Cortical bone	13,700	0.3
Cancellous bone	7,930	0.3

Table 2: Material parameters for the cortical and cancellous bone

3.5 Muscles

The muscles of the masticatory system can be classified into the categories opening and closing muscles. The jaw openers are the lateral pterygoid and the digastric. The jaw closers are the masseter,

temporalis and medial pterygoid. These muscles have been included into our model. Initially, the remaining suprahyoid muscles were included, but were suppressed since they restrict the anterior movement of the mandible. The realistic opening motion obtained after their removal confirms that they don't play a fundamental role opening the jaw.
Muscles are divided into two parts: the fiber and the tendon. In our model, we use a Hill muscle model to represent the fiber and an inextensible wire to represent the tendon. The tendon undergoes very small deformation and can thus be neglected. The muscles are represented in our model in the following manner: Anterior and posterior temporalis, superficial and deep masseter, superior and inferior lateral pterygoid, medial pterygoid and digastric.
The forces produced by the muscles are principally regulated by the sarcomeres, the contractile units of the myofibrils. These forces are influenced by the length of the sarcomeres (force-length relationship) and their contraction velocities (force-velocity relationship). Additionally, the muscle generates a passive elastic force during stretching. These characteristics are represented by the Hill type muscle model following van Ruijven & Weijs [24], where the force is expressed as

$$F(t) = F_{\max}[A(t)FL(t)FV(t) + FP(t)]. \tag{2}$$

F_{max} is the maximum isometric muscle force, A(t) the instantaneous activation level, FL(t) is the force-length factor, FV(t) the force-velocity factor, and FP(t) the parallel elastic force.
The instantaneous sarcomere length is defined as

$$Ls(t) = \{Lm(t) - (Lm_i - Lf_i)\}\{\frac{Ls_i}{Lf_i}\}, \tag{3}$$

where $Lm(t)$ is the instantaneous muscle length, Lm_i the initial muscle length, Lf_i the initial muscle fiber length and Ls_i the initial sarcomere length. The origin and insertion points of the muscles were determined directly from the geometry of our model. The values of Lm_i, Lf_i and Ls_i were obtained from van Eijden et al. [25].
The sarcomeres can only function inside a determinate range, progressively losing capacity to exert force as the length moves away from the optimal length. In this optimal length, a muscle can produce its maximum isometric force F_{max}. A force-length factor as a function of the sarcomere length $Ls(t)$ is introduced as (since this factor is an approximation, the last digits of each term are not necessary)

$$FL(t) = 0.412Ls(t)^3 - 4.3957Ls(t)^2 + 14.8003Ls(t) - 15.0515 \tag{4}$$

. Additionally, during concentric contraction, sarcomeres are able to produce less force than during isometric contraction. On the other hand, muscles can produce their maximum force during eccentric contraction. This phenomena is taken into account by the force-velocity factor, defined as

$$FV(t) = \begin{cases} \left\{\dfrac{12.5 - (\dfrac{Vs(t)}{2.73})}{12.5 + (\dfrac{Vs(t)}{0.49})}\right\}, & Vs(t) \geq 0 \\ 1.5 - 0.5\left\{\dfrac{12.5 + \dfrac{Vs(t)}{2.73}}{12.5 - \left(\dfrac{Vs(t)}{2.73}\right)}\right\}, & Vs(t) < 0 \end{cases}. \tag{5}$$

Finally, the parallel elastic force has the following expression

$$F(t) = 0.0014\exp\left(6\frac{Ls(t) - 2.73}{2.73}\right). \tag{6}$$

The maximum force a muscle can generate is obtained by multiplying its physiological cross-sectional area (PCSA) with the value of 40 N/cm^2 [26]. The PCSA of each masticatory muscle was obtained from van Eijden et al. [25].

4 Simulations

4.1 Jaw Opening

Jaw opening was achieved by activating the lateral pterygoid and digastric muscle during an interval of 75 ms. The TMJ undergoes a realistic behavior during jaw opening as shown in Figure 2, i.e. a rotational motion is followed by a translational one in the condyle. A gap of 35 mm between the incisive teeth was achieved when reaching an activation level of 100% for the opening muscles. This gap is slightly lower than the natural range of maximum mouth opening [27] which is around 45.3 +/- 5.7 mm for adult men. The gap is limited in our model by the approach to fix the position of the hyoid bone, resulting in the digastric muscle quickly losing capacity to generate force as it contracts.

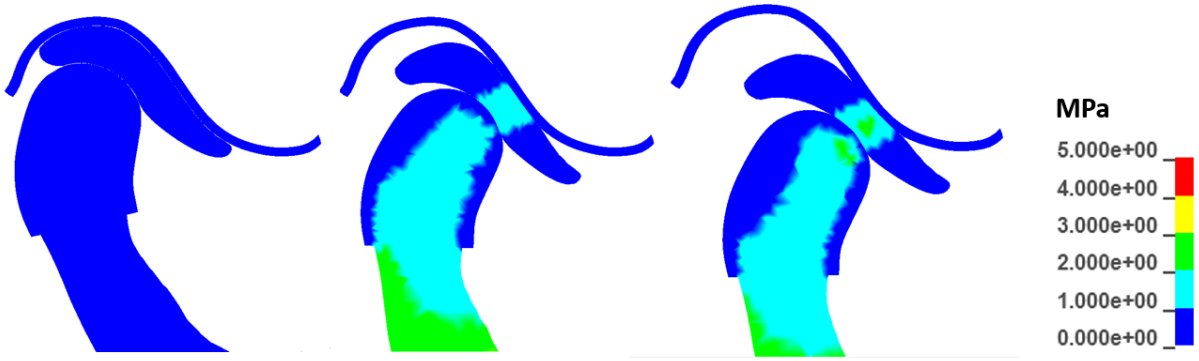

Fig.2: Stress distribution in the TMJ during opening.

Resulting forces in the TMJ during jaw opening are similar to those obtained by Koolstra & van Eijden [2]. The joint forces in our model are somewhat lower since Koolstra's model includes the rest of the suprahyoid muscles (mylohyoid, geniohyoid). The resulting joint force is displayed in Figure 3.

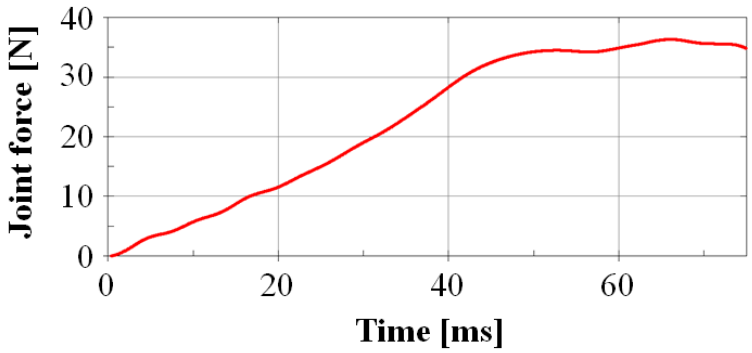

Fig.3: Forces in the joint during opening

Due to the action of the lateral pterygoid muscle during opening, stresses in the mandible are almost completely compressive on the inner surface and tensile on the outer surface. In Figure 4, a lateral view of the jaw with the first principal stresses and a medial view with the third principal stresses are shown. The highest tensile stresses can be observed in the lateral side of the ramus while notable tensile stresses can be observed in the mandibular notch and the outer surface of the mandibular body. The highest compressive stresses are found in the posterior part of the ramus while notable compressive stresses are seen in the inner surface of the mandibular body.

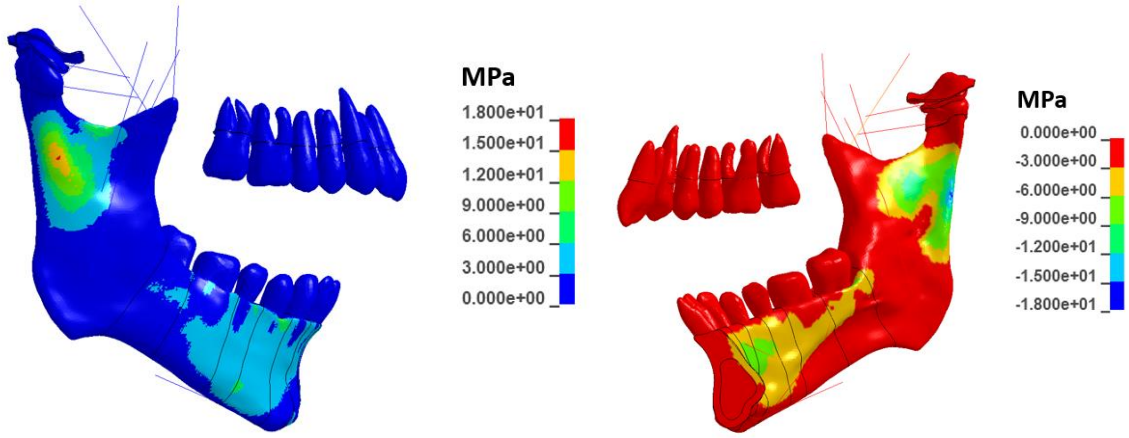

Fig.4: First (left) and third (right) principal stresses in the jaw during opening

4.2 Biting tasks

For bilateral biting tasks only half of the jaw is required while applying classical symmetry boundary conditions. However, initial trials where all closing muscles were activated at the same levels resulted in the mandible not finding an equilibrium position. Furthermore, the condyle can displace out of the mandibular fossa since the forces in the posterior direction are very large. Additionally, the bolus may not remain between the designated teeth during biting tasks. However, the activation levels provided by Rues et al. [28], resulted in these tasks being successfully completed. It was, however, necessary to bring the lateral pterygoid muscle to high activation levels to reach balance. Posterior introduction of the inferior retrodiscal tissue allowed us to both, a) the reduction of the role of the lateral pterygoid muscle in order to obtain balance, and b) additionally the achievement of higher biting forces. Resulting forces in the TMJ show now very good agreement with the theoretical forces calculated by Rues et al [28]. Figure 5 presents the biting and joint forces obtained during a bilatelar molar biting (BMB) task in a period of 250 ms with a 10x10x10 (mm) bolus.

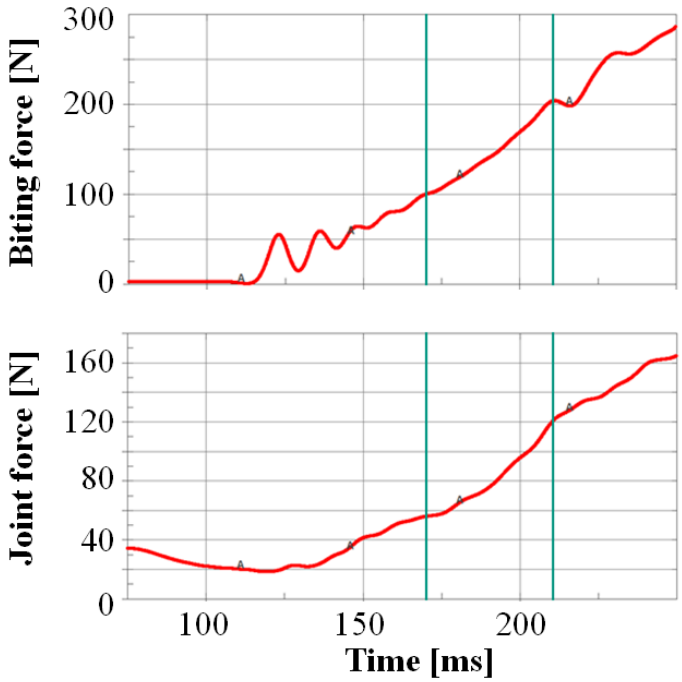

Fig.5: Biting and joint forces during bilateral molar biting.

In Figure 6 we can see the first principal stress under a bite force of 300 N. The third principal stress is shown in Figure 7. Areas under high tension in the jaw include the posterior part of the mandibular notch, the coronoid process and the anterior border. The posterior part of the ramus is the area under highest compression. Compression can also be observed in the posterior part of the coronoid process. These

areas of tension and compression agree with those obtained by Korioth et al. [29] and Kober et al. [30]. Some discrepancies are visible, however, in the tension present on the coronoid process, which is absent in Kober's model. Nevertheless, a direct comparison cannot be made since unilateral premolar biting tasks have not yet been performed with our model. A linear relationship between bite force and the maximum von Mises stress in the model can be seen in Table 3.

Bite force [N]	Von Mises stress[MPa]
300	34
800	89

Table 3: Maximum von Mises stress for bilateral molar biting.

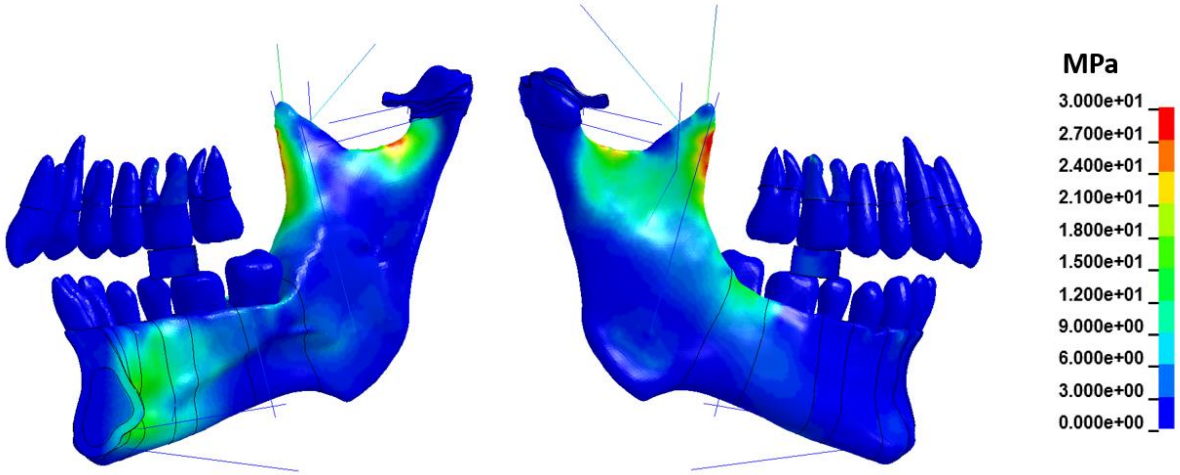

Fig.6: First principal stress during bilateral molar biting. Medial (left) and lateral view (right).

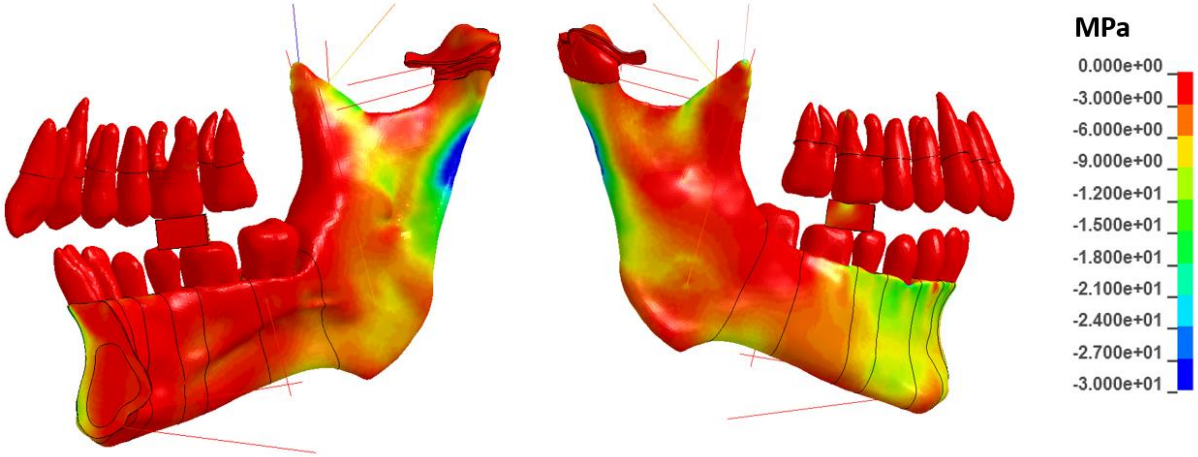

Fig.7: Third principal stress during bilateral molar biting. Medial (left) and lateral view (right).

In order to be able to compare our results more closely with those of Korioth [29], a unilateral molar biting task was performed calibrating the forces to obtain a similar joint/bite force ratio. In Figure 8, the first principal stresses of the jaw are depicted for unilateral molar biting. Here a 10x10x2 (mm) bolus was placed between the molars, and the muscle forces increased until a bite force of 300 N was reached. The third principal stresses can be seen in Figure 9.

A discrepancy can be observed, since for a biting force of 526N the maximum values for both first and third principal stresses reported by Korioth et al. [29] are of approximately 25 MPa. In our model, these

values are surpassed with a bite force of 300 N. The obtained results are, however, still below the ultimate tensile stress (135 MPa) and the ultimate compressive stress (205 MPa) of the bone [31].

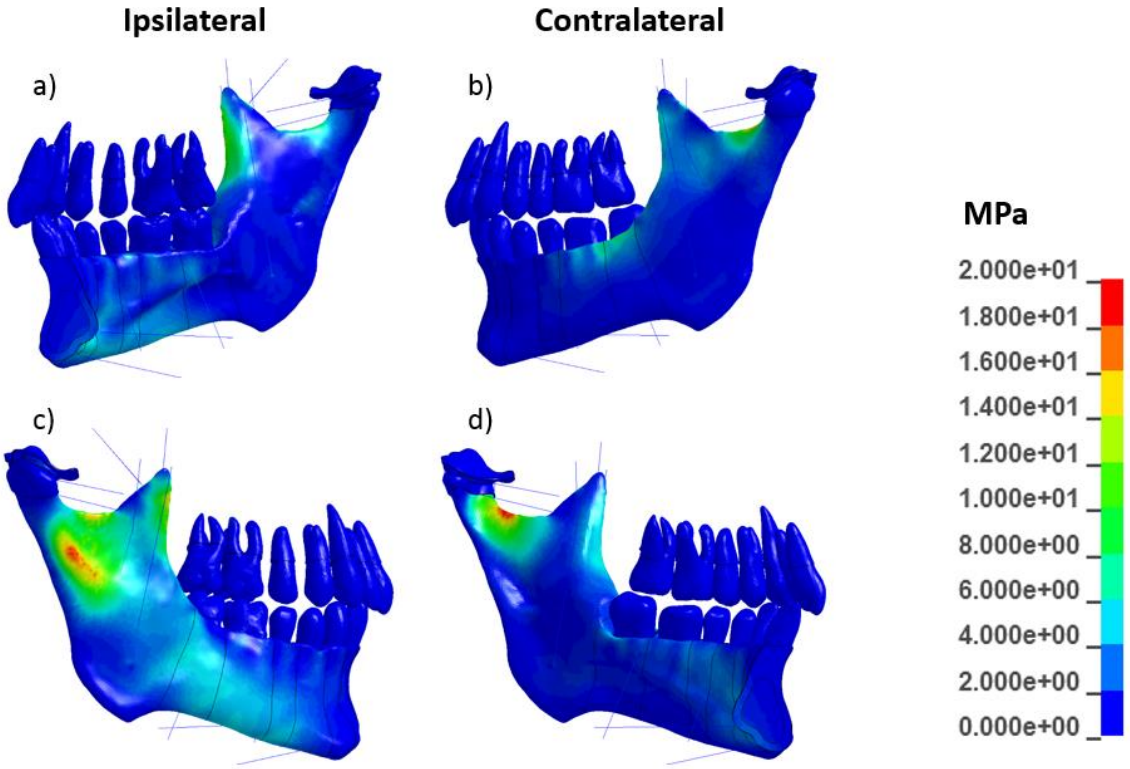

Fig.8: First principal stress in the jaw: a) medial view ipsilateral side, b) lateral view contralateral side c) lateral view ipsilateral side and d) medial view contralateral side under a unilateral molar bite force of 300 N.

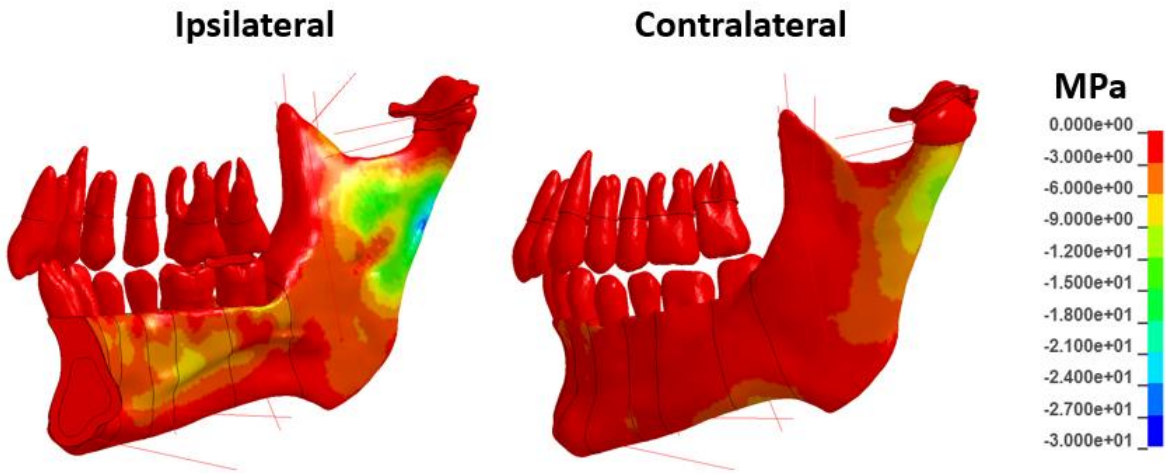

Fig.9: Third principal stress in the jaw in the ipsilateral (medial view) and contralateral side (lateral view) under a unilateral molar bite force of 300 N.

5 Discussion of results

5.1 Jaw opening

Initial simulations where the mylohoid and geniohyoid muscles were included resulted in the condyle being unable to displace anteriorly. They were thus not considered, in order to obtain a realistic motion during opening. The combined forces in the posterior direction of the suprahyoid muscles are larger than the force produced by the lateral pterygoid. Moreover, the digastric muscle is capable of opening the jaw and reaching maximum mouth opening on its own.

5.2 Biting tasks

Data of the distribution of forces during biting tasks vary considerably in the literature. This results mainly from the difference in angle and application point of the muscle forces between authors. Throckmorton [28] shows that modifying the muscles parameters gives a range of 3.8-12.5 kg of joint force for a biting force of 20 kg. Our model is calibrated to match the results from Rues et al. [] since these biting and muscle forces were experimentally measured. It must be noted, however, that different activation levels of the temporalis and the masseter can significantly reduce forces on the joint. Initial simulations required the use of the lateral pterygoid to stabilize the condyle during biting tasks. As the biting force increased, the action of the lateral pterygoid increased as well. The maximum biting force was limited by the capacity of the lateral pterygoid to stabilize the condyle, this limit being reached with the closing muscles still being able to produce much larger forces. The introduction of the anterior and posterior attachments of the disc allowed us to reduce the role of the lateral pterygoid during moderate biting forces (0 – 300 N) and to use most of the potential of the muscles during strong biting forces (> 400 N).
Simulations where the bite force is notably larger than in the joint, require an orientation of the total force of the closing muscles towards the anterior direction. This necessitates that the joint force exerted on the condyle possesses a large posterior component in order to reach balance. In a static model, this balance is easily reached since the condyle is completely constrained. In our dynamic model, however, joint forces are restricted to the normal direction of the fossa. This type of reaction force results in a very unstable position of the disc, since an increase of the posterior forces (mild activation of the posterior temporalis) results in the disc quickly displacing to its maximum posterior position (left picture in Figure 2). This is the most stable position of the disc, since the temporomandibular ligament and the attachments of the disc ensure that no further posterior displacement is possible. This observation suggests that joint forces have a considerable effect on the stabilization of the articular disc during high biting forces.

Discrepancies in the maximum von Mises stress in comparison to results of other authors can be caused by several reasons: Stresses in the coronoid process are very sensitive to the angle at which the temporalis muscle applies its force. Since the complete skull was not available in our DVT-scans, the origin point of the temporalis muscle was determined with coordinates available in the literature. Further, differences in the geometries of the models can also contribute to this discrepancy, but most importantly, Korioth's model incorporates the anisotropy of the bone, which according to Kober et al. [30] reduces the stress in the jaw. The introduction of bone anisotropy into our model is one of the current goals.

6 Computational requirements of the model

Due to the size of the model, simulations are executed in the "InstitutsCluster II" of the KIT. Table 4 shows the required computational time for a model with 1,840,000 elements (mostly tetrahedral, resulting in 1,164,000 degrees of freedom) and a problem time of 75 ms executed with LS-DYNA mpp R.6.1.1. This is the complete model used during unilateral molar biting. For bilateral biting, a model with half the number of elements is employed. Simulations may require a problem time of 75 to 500 ms depending on the type of task being analyzed.

#CPU	Computational time	Scaling
16	32 hours 28 minutes	1.0
32	14 hours 14 minutes	2.28
64	8 hours 38 minutes	3.76

Table 4: Computational requirements for the complete model

Increasing the number of processors from 16 to 32 gives very good results, increasing the efficiency of the computation (scaling is greater than two with twice the number of processors). Further rising the number of processors continues to reduce the computational time, but overall computational efficiency is only slightly reduced. In our model, very small elements are required to properly mesh the PDL, which limits the size of time step. The use of mass scaling would allow great reduction of the computational time, it was, however, not used in the simulations shown in Table 4. It is, on the other hand, used during the calibration of new tasks, resulting in greatly reduced computational times.

7 Summary

A dynamic finite element model of the overall human masticatory system has been developed with the goal to overcome the limitations and computational problems arising from modeling the system as a static problem. Dynamic modeling of the system requires that muscle activation is precisely known in order to obtain a stable position of the bolus and the articular disc during biting tasks. The model shows that a proper jaw opening is obtained through activation of the digastric and lateral pterygoid muscles. Introduction of the geniohyoid and mylohyoid muscles produces forces towards the posterior direction that inhibit the anterior displacement of the disc. The high capacity of the temporalis muscle to produce forces in the posterior direction requires the inclusion of the posterior and anterior attachments of the disc and of the temporomandibular ligament to ensure the stability of the joint during strong forces. The current model can recreate most of the results found in the literature and shows reasonable levels of stress in the different components of the masticatory system. The model can be used to perform miscellaneous studies in the field of dental science. Currently the aim is to evaluate changes in the behavior of the stomatognathic system when implants are introduced, and to evaluate the effect of parafunctional activities such as bruxism.

8 Literature

[1] Fill, T.S., Toogood, R.W., Major, P.W and Carey, J.P.: "Analytically determined mechanical properties of, and models for the periodontal ligament: Critical review of literature", Journal of Biomechanics 45, 2012, 9-16

[2] Koolstra, J. H. and van Eijden, T.M.G.J.: ”Combined finite-element and rigid-body analysis of human jaw joint dynamics”, Journal of Biomechanics 38, 2005, 2431-2439

[3] Rues, S., Lenz, J., Türp, J.C., Schweizerhof, K. and Schindler, H.J.: Muscle and joint forces under variable equilibrium states of the mandible“, Clin Oral Investig. 15 (5), 2011, 737-47

[4] Livermore Software technology Corporation: LS-DYNA 6.1 Manual, 2011

[5] Langenbach, G.E.J. and Hannam, A.G.:. “The role of passive muscle tensions in a three-dimensional dynamic model of the human jaw”, Archives of Oral Biology 44, 1999, 557-573.

[6] Martinez, S., Schweizerhof, K., Schindler, H.J and Lenz, J.: “Abschlussbericht: Erstellung eines Finite Elemente (FE) Modells des Unterkiefers zur Ermittlung der unter funktionellen (und ggfs. dysfunktionellen) Belastungen auftretenden Deformationen sowie der Verschiebungen der Zähne“,2014.

[7] Materialise N.V, Mimics 14.12, Reference guide, 2011.

[8] 3D Systems, Geomagic Studio 12, Reference guide, 2010.

[9] Altair, Hyperworks 12, Reference guide, 2013.

[10] Nishihira, M., Yamamoto, K., Sato, Y., Ishikawa, H. and Natali, A.N..: “Mechanics of periodontal ligament”, Dental Biomechanics, London: Taylor & Francis, 2003.

[11] Huang, H., Tang, W., Yan, B. and Wu, B.: “Mechanical responses of Periodontal Ligament under a realistic orthodontic loading”. Procedia Engineering 31, 2012, 828–833.

[12] Natali, A.N., Pavan, P. G. and Scarpa, C.: “Numerical analysis of tooth mobility: formulation of a non-linear constitutive law for the periodontal ligament”. Dental Materials 20, 623–629, 2004.

[13] Parfitt, G. J.: “Measurement of the Physiological Mobility of Individual Teeth in an Axial Direction”. J Dent Res 39, 1960, 608-618.

[14] Lenz, J., Schindler, H. J. and Pelka H.: “Die keramikverblendete NEM-Konuskrone“. Berlin: Quintessenz-Verl. GmbH, 1992.

[15] Limbert, G., Middleton, J., Laizans, J., Dobelis, M. and Knets I.: “A transversely isotropic hyperelastic constitutive model of the PDL. Analytical and computational aspects”, Computer Methods in Biomechanics and Biomedical Engineering 6, 2003, 337–345.

[16] Pietrzak, G., Curnier, A., Botsis, J., Scherrer, S., Wiskott, A. and Belser U.: “A nonlinear elastic model of the periodontal ligament and its numerical calibration for the study of tooth mobility”, Computer Methods in Biomechanics and Biomedical Engineering 5, 2002, 91–100.

[17] Su, M. Z., Chang, H. H., Chiang, Y. C., Cheng, J. H., Fuh, L. J., Wang, C. Y. and Lin, C. P.: "Modeling viscoelastic behavior of periodontal ligament with nonlinear finite element analysis", Journal of Dental Sciences 8, 2013, 121-128.
[18] Perez del Palomar, A. and Doblare, M. "The effect of collagen reinforcement in the behavior of the temporomandibular joint disc". Journal of Biomechanics 39, 2006, 1075–1085.
[19] Koolstra, J.H. & van Eijden, T.M.G.J.: "Consequences of Viscoelastic Behavior in the Human Temporomandibular Joint Disc". J Dent Res 86, 2007, 1198-1202.
[20] Tanaka, E., Hanaoka, K., Tanaka, M., van Eijden, T., Iwabe, T., Ishino, Y., Sasaki, A. and Tanne K.: "Viscoelastic properties of bovine retrodiscal tissue under tensile stress-relaxation", Eur J Oral Sci 111, 2003, 518–522.
[21] Odin, G. & Savoldelli, C. & Bouchard, P. & Tillier, Y.: "Determination of Young's modulus of mandibular bone using inverse analysis", Medical Engineering and Physics 32, 2010, 630-637.
[22] Lettry, S., Seedhom, B.B., Berry, E. and Cupponea, M.: "Quality assessment of the cortical bone of the human mandible", Bone 32, 2003, 35–44.
[23] Tanaka, E., Rodrigo, D. P., Tanaka, M., Kawaguchi, A., Shibazaki, T. and Tanne, K.: "Stress Analysis in the TMJ during Jaw opening by use of a three-dimensional Finite Element Model based on magnetic resonance Images", International Journal of Oral and Maxillofacial Surgery 30, 2001, 421-430.
[24] van Ruijven, L. J. and Weijs, W.A.: "A new model for calculating muscle forces from electromyograms". European Journal of Applied Physiology 61, 1990, 479–485.
[25] van Eijden, T.M.G.J., Korfage, J.A.M. and Brugman, P.: "Architecture of the Human Jaw-Closing and Jaw-Opening Muscles", The Anatomical Record 248, 1997, 464–474.
[26] Weijs, W.A. and Hillen, B.: „Cross-sectional areas and estimated intrinsic strength of the human jaw muscles", Acta Morphol. Neerl.-Scand 23, 1985, 267-274.
[27] Sawair, F.A., Hassoneh, Y.M., Al-Zawawi, B.M. and Baqain Z.H.: "Maximum mouth opening. Associated factors and dental significance", Saudi Med J 4, 2010, 369-373.
[28] Rues, S., Lenz, J., Türp, J. C., Schweizerhof, K. and Schindler, H. J.: "Muscle and joint forces under variable equilibrium states of the mandible", Clin Oral Investig. 15(5), 2011, 737-47.
[29] Korioth, T.W.P., Romilly, D. P. and Hannam A. G.: "Three-Dimensional Finite Element Stress Analysis of the Dentate Human Mandible", American Journal of Physical Anthropology 88, 1992, 69-96.
[30] Kober, C., Erdmann, B., Hellmich, C., Sader, R. and Zeilhofer H.F.: "Anisotropic Simulation of the Human Mandible", 17th ASCE Engineering Mechanics Conference, 2004.
[31] Reilly, S.B. and Burstein, A.H..: "The elastic and ultimate properties of compact bone tissue", J Biomechan 8, 1975, 393-405.
[32] Throckmorton G. S.: "Quantitative calculations of temporomandibular joint reaction forces-II. The importance of the direction of the jaw muscle forces", J Biomechanics 18, 1985, 453-461.